

SDRP Journal of Earth Sciences & Environmental Studies (ISSN: 2472-6397)

Mechanism and identify photolysis products of fluopyram under TiO₂: Experiments, DFT and *ab initio* Molecular dynamics study

Jiye Hu*, Kyongjin Pang, Bizhang Dong

DOI: 10.25177/JESSES.4.3.RA.504

Research

Received Date: 15th Apr 2019Accepted Date: 01st May 2019Published Date: 05th May 2019

Copy rights: © This is an Open access article distributed under the terms of International License.



School of Chemistry and Biological Engineering, University of Science Technology
Beijing, Beijing, 100083, PR China

CORRESPONDING AUTHOR

Jiye Hu,

Tel: +86 82376002 Fax: +86 1082376002

E-mail address: jyhu@ustb.edu.cn (Jiye Hu), banggyongjin@163.com (Kyongjin Pang)

CITATION

Jiye Hu, Kyongjin Pang, Bizhang Dong, Mechanism and identify photolysis products of fluopyram under TiO₂: Experiments, DFT and *ab initio* Molecular dynamics study (2019) SDRP Journal of Earth Sciences & Environmental Studies 4(3) p:681-690

ABSTRACT

Fluopyram is one of the widely used fungicides and it is persistence in water and soil. In this study, the photocatalytic degradation of fluopyram by TiO₂ was investigated under simulated solar light irradiation. Six transformation products (TPs) were identified by means of high performance liquid chromatography coupled with tandem mass spectrometry (HPLC-MS/MS) and the quantum chemistry calculations (DFT and AIMD method). The formation of these TPs involved the hydroxyl-substitution of Cl atom, intramolecular cyclization, cleavage of amido bond, loss of trifluorotoluene, and attack of hydroxyl group on benzene ring. And then, a tentative pathway of the photocatalytic degradation was proposed. The toxicity of fluopyram and its TPs were predicted using *in silico* test. The results showed that potentially more toxic intermediates formed during photocatalytic degradation. These data suggested that more information about TPs of fluopyram and their toxicity should be obtained.

Keywords: Fluopyram, Photocatalytic degradation, Toxicity, DFT, AIMD

1. INTRODUCTION

Fluopyram (N-(2-[3-chloro-5-(trifluoromethyl)-2-pyridinyl]ethyl)-2-(trifluoromethyl)benzamide), is a new broad-spectrum fungicide belonging to the class of succinate dehydrogenase inhibitors. Fluopyram is non-toxic to mammals, birds, honeybees and duck, slightly toxic to daphnia and freshwater green algae, and moderately toxic, even highly toxic to freshwater fish and marine species (The Health Canada Pest Management Regulatory Agency 2014). Fluopyram is an endocrine disrupting compound on the endocrine systems of human beings and wildlife at trace level (Rouquié et al. 2014; Tinwell et al. 2014). In addition, it has a negative effect on overall soil microbial activity and changes soil microbial community structure and function (Zhang et al. 2014). In soils, fluopyram is persistent and has a potential for long-term accumulation and residue carry over to the following crop season (The Health Canada Pest Management Regulatory Agency 2014).

Although in our previous study, the photolysis of fluopyram has been studied under the various environmental condition such as exist pH, TiO_2 , NO_x^- and Fe(III) (Dong and Hu 2016), it have not identified the photolysis products of fluopyram in much details when exist TiO_2 . In addition, TP I is one of the main photolysis product of fluopyram that was containing 8-membered cyclic organic compound. No previous study has investigated the mechanism to formation 8-membered cyclic organic compound under the room temperature in water.

Heterogeneous photocatalysis has been proven to be effective for the degradation of a variety of toxic substances, including insecticides, fungicides and herbicides, under artificial or solar irradiation (Berberidou et al. 2015; Stamatis et al. 2015). However, many target compounds were not completely mineralized during the photocatalytic reaction time (Šojić et al. 2009; Yang et al. 2010). Diverse studies have proven that some of pesticide TPs, including the photocatalytic by-products, are more abundant, toxic and/or persistent than their parent compounds (Boxall et al. 2004; Martínez Vidal et al. 2009; Postigo et al. 2011a, b; Šojić et al. 2014; Berberidou et al. 2015).

Quantum chemistry calculation using density functional theory (DFT) was extensively used to complement the experimental result due to that provides a clear elucidation for the reactive center or breakage of chemical bond such as atomic charges, natural bond orbitals (NBO) and bond order of molecular structures (Jung et al. 2018). Ab initio molecular dynamics (AIMD) method were considered a state-of-the art approach to describe the chemical processes in solution (Govindarajan 2018, Pavlova 2012). In present study, DFT and AIMD method were carried out to illustrate the translation reaction of Fluopyram in water.

The objectives of this work were therefore to (i) identify the TPs of fluopyram issued from photocatalytic degradation in 100 mg L^{-1} TiO_2 suspensions under simulated solar light irradiation using HPLC-MS/MS and the DFT method, (ii) propose a photocatalytic degradation pathway and describe the degradation pathway using DFT and AIMD method, and (iii) assess the potential toxicity of the resulting TPs using an *in silico* quantitative structure-activity relationship (QSAR) approach.

2. METHODOLOGY

2.1 Experimental details

Fluopyram (99.4% purity) was obtained from the Sigma-Aldrich Trading Co., Ltd (Shanghai, China). Chromatographic grade acetonitrile and acetone was purchased from Thermo Fisher (Beijing, China). Ultrapure water was prepared by a Milli-Q system (Bedford, USA). TiO_2 Degussa P25 (80% anatase and 20% rutile form, $50 \text{ m}^2 \text{ g}^{-1}$, about 30 nm) was used for the degradation experiments. Due to the poor solubility of fluopyram in water (16 mg L^{-1} at 25°C), a standard stock solution of fluopyram at 1000 mg L^{-1} was prepared in acetone.

Photocatalytic experiments were carried out with a home-made photochemical reactor equipped with a 500-W xenon lamp delivering radiation at wavelengths of 300 to 800 nm, which was positioned in the center of the reactor. The radiation intensity was 200 W m^{-2} ($720 \text{ KJ m}^{-2} \text{ h}^{-1}$). In order to easily find and identify the TPs, 2 mL the standard stock solu-

tion after removing acetone was redissolved with 100 mL 1% acetonitrile-water (v/v) to achieve 20 mg L⁻¹ fluopyram solution. Based on our previous research (Dong and Hu, 2016), the concentration of TiO₂ was set as 100 mg L⁻¹. In order to maintain the catalyst in suspension, the aqueous solution at pH 7.5 was irradiated in capped glass tube with magnetic stirring. The distance between the tube and xenon lamp was 30 cm, which ensured the normal operation of magnetic stirrer. An aliquot of 1 mL reaction solution was taken at the intervals of 0, 1, 3, 5, 7, 14, 21, 30, 45 d and filtered through syringe filters (0.22 µm) (Bonna-Agela Technologies, Tianjin, China) to remove TiO₂ particles before further analysis. Dark control wrapped in aluminum foil was run simultaneously under the same condition.

TPs were analyzed by an Agilent 1260 HPLC coupled to an Agilent 6420 triple quadrupole mass spectrometer with electrospray ionization source (ESI). An Agilent SB-C18 analytical column (50 mm × 3.0 mm i.d., 2.7 µm) was used for separation of TPs and was maintained at 30 °C. The mass spectrometer was operated under positive/negative ionization mode. The mobile phase was a mixture of water and acetonitrile flowing at 0.3 mL min⁻¹ in gradient elution conditions: The percentage of acetonitrile was 35% at 0 min and maintained for 1.5 min, increased to 80% at 3.0 min and hold for 1.0 min, then returned to the initial 35% acetonitrile at 6.0 min and kept for 5 min. The mass spectroscopy (MS) detection conditions were as followed: drying gas temperature was 350 °C, drying gas flow was 10 L min⁻¹, and nebulizer gas (N₂) pressure was 45 psi. MS/MS scan mode was conducted at fragment voltage of 135 eV with mass scan range of 50-500 amu at preliminary screening of products. In the MS/MS experiments, the collision energy (CE) for each compound was held at 20 eV with mass scan range of 50-500 amu.

2.2 Computational details

Structural optimization and natural charges of fluopyram and its Tps were performed by Gaussian 09 at B3LYP/6-311++G(2d, 2p) level of DFT (Frisch et al., 2013), and bond order calculated by DMOL³ module

in Material Studio 8.0 at DFT/meta-GGA exchange-correlation function (basis set DNP and basis file 4.4) (Roberto and Donald, 2012).

For ab initio molecular dynamics (AIMD) simulations, the 3D periodic box (23.8 × 23.8 × 23.8 Å³) containing 8 optimized Fluopyram and 256 water molecules was constructed by Amorphous Cell module with universal Forcefield, Electrostatic and van der waals's interaction based on the atom and 12.5 Å cut off distance, where the density of the amorphous cell was 0.98 g/cm³. The electron exchange and correlation energies are carried out the generalized gradient approximation of the Perdew-Burke-Ernzerhof (GGA-PBE) functional (Perdew, 1996). The AIMD simulation with canonical ensemble (NVT, constant number of atoms, volume, and temperature) is performed with a time step of 1 fs in a period of 10 ps, 2 × 2 × 2 Monkhorst-Pack k-point mesh (Monkhorst and Pack, 1976), a cutoff energy of 520 eV and temperature of 300 K. Then, the AIMD simulation with canonical ensemble (NVE, constant number of atoms, volume, and energy) is performed using the after result model of NVT ensemble.

Aquatic toxicity, bioaccumulation factors (BCFs), mutagenicity, developmental toxicity (DT) and acute toxicity to rat of the identified TPs as well as the parent compound were predicted with the ECOSAR v.2.0 and T.E.S.T. v.4.1, which were U.S. Environmental Protection Agency online available toxicity predictive system with QSAR mathematical models.

3. RESULTS AND DISCUSSION

3.1. Identify of the TPs by HPLC-MS/MS

The total ion chromatograms (recorded in the full scan mode) obtained after HPLC-MS/MS analysis are shown in Fig. 1. Six photocatalytic products were identified on the basis of the mass shifts from the parent molecule, the presence of the peak of the protonated molecule and sodium adduct, the isotopic pattern in the molecular ion and the interpretation of MS/MS spectra (Dong and Hu, 2016) and referred as TP I to TP VI.

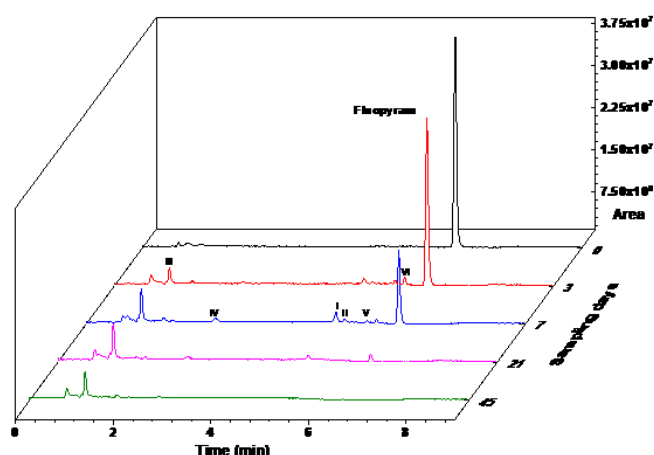


Fig. 1. TIC of the fluopyram solution irradiated in different sampling intervals

The retention times and fragment ion of MS/MS of each compound are given in Table 1. TP I was identified as 2,9-bis(trifluoromethyl)-6,7-dihydrobenzo[c]pyrido[3,2-e]azocin-8 (5H)-one and TP II was N-(2-[3-hydroxy-5-(trifluoromethyl)-2-pyridinyl]ethyl)-2-trifluoromethylbenzamide, both which were also

found and identified in photolysis of fluopyram (Dong and Hu 2016). The monoisotopic mass of TP III, TP IV, TP V and TP VI were 224, 252, 412 and 412, respectively, on basis of $[M + H]^+$ and/or $[M + Na]^+$ (Table 1).

It was concluded that the molecule of the four compounds contain one chlorine and even or zero nitrogen atom on basis of the even molecular weight and intensity of the $A + 2$ isotopic peaks. These compounds were corroborated by the MS/MS fragmentation spectra observed during product ion scan analysis. TP III and TP IV were identified as 3-chloro-5-(trifluoromethyl)-2-ethylamino-pyridine and 3-chloro-5-(trifluoro-methyl)-2-ethylformamide-pyridine, respectively. TP V and TP VI were hydroxyl group substitution products. The MS/MS fragment ion of TP V and TP VI were compared, the results showed that the nucleophilic substitution taken place on the benzene ring of fluopyram.

Table 1: Retention times (R_t) and elemental composition of fragment ions of fluopyram and its TPs

| Compound | R_t (min) | Elemental composition | Fragment ion (m/z) |
|-----------|-------------|---------------------------|--|
| Fluopyram | 6.41 | $C_{16}H_{12}ClF_6N_2O$ | 419, 397, 208, 173, 145 |
| TP I | 5.12 | $C_{16}H_{11}F_6N_2O$ | 383, 361, 343, 341, 332, 321, 316, 312 |
| TP II | 5.30 | $C_{16}H_{13}F_6N_2O_2$ | 401, 379, 190, 173, 170 |
| TP III | 1.14 | $C_8H_9ClF_3N_2$ | 225, 196, 208, 172 |
| TP IV | 2.66 | $C_9H_9ClF_3N_2O$ | 275, 253, 225, 208, 196, 172 |
| TP V | 5.77 | $C_{16}H_{12}ClF_6N_2O_2$ | 435, 413, 208, 189 |
| TP VI | 5.95 | $C_{16}H_{12}ClF_6N_2O_2$ | 435, 413, 225, 208, 189 |

But the attacked positions were unclear on the benzene ring of fluopyram because the same molecular fragment (m/z 208) was detected for TP V and TP VI. In order to clarify the position of the hydroxy substitution, DFT study was carried out and the results showed in section 3.2. And the formation of molecular fragment (m/z 225) suggested that the substitution of hydroxyl had an effect on fragmentation of TPs.

3.2. Analysis of NBO for Fluopyram

The positions of the hydroxy addition on the benzene

ring were further verified using the quantum chemistry calculations (Fig. 2).

The natural charges of C atoms on the benzene ring was shown at Fig. 2. As shown in Fig. 2, on the benzene ring, the natural charges of the C2 and C5 atoms were 0.220 and 0.010 with positive values and C3 and C4 atoms were -0.239 and -0.274, respectively. The bond orders of the CO and benzene bonds (labeled B_{CO-Ar}), and CH_2 and NH bond (labeled B_{CH_2-N}) were also calculated by DFT/meta-GGA (M11-L) on the basis set of DNP and basis file 4.4.

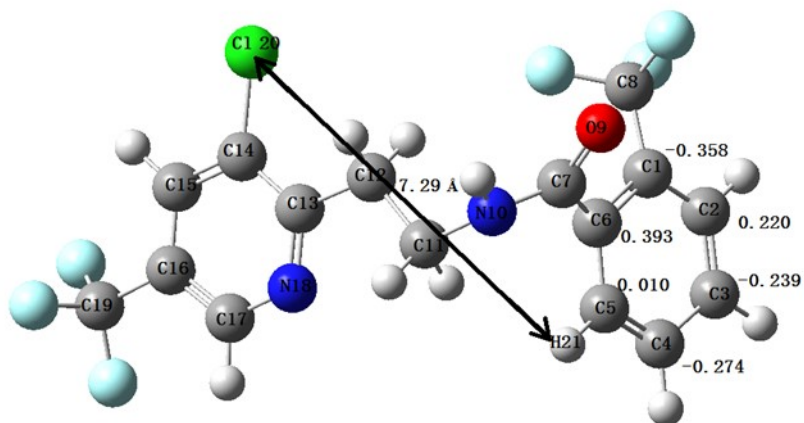


Fig. 2. Optimized structure of fluopyram at B3LYP/6-311++G(2d, 2p) level of DFT

Note: Distance between Cl (20) and noted H (21) atom is 7.29 Å, natural charges of the C atoms on the benzene ring was presented.

The results showed that OH-5 more hardly degraded to small molecular with higher bond order of B_{CO-Ar} and B_{CH2-N} (Table 2). Therefore, it can be considered that the $-OH$ group mainly attack to C2 and C5 atoms on the benzene with positive values.

Table 2: The bond order values calculated by DFT/meta-GGA (M11-L) on the basis of DNP 4.4 level of theory for four possible hydroxylation products

| Hydroxylation products | B_{CO-Ar} | B_{CH2-N} |
|------------------------|-------------|-------------|
| OH-2 | 0.764 | 0.828 |
| OH-3 | 0.764 | 0.831 |
| OH-4 | 0.764 | 0.829 |
| OH-5 | 0.775 | 0.832 |

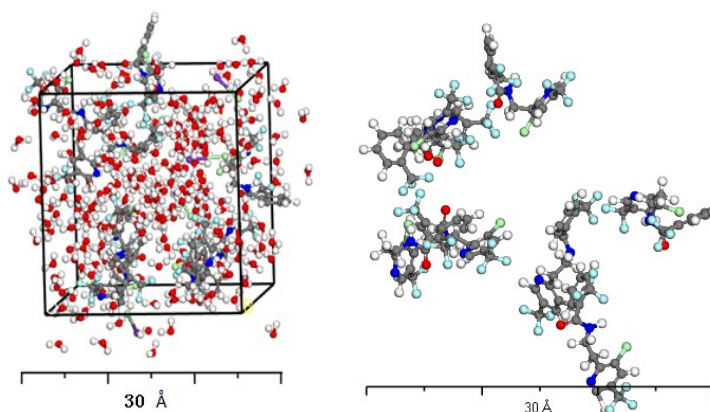


Fig. 3. Ab initio molecular simulation using DFT/GGA/PBE on the basis of DNP 4.4 level of theory, (a) initial stage and (b) after 10 ns dynamics.

Note. Red fragments present the water molecular in (a), and water and cubic grid was not presented in (b)

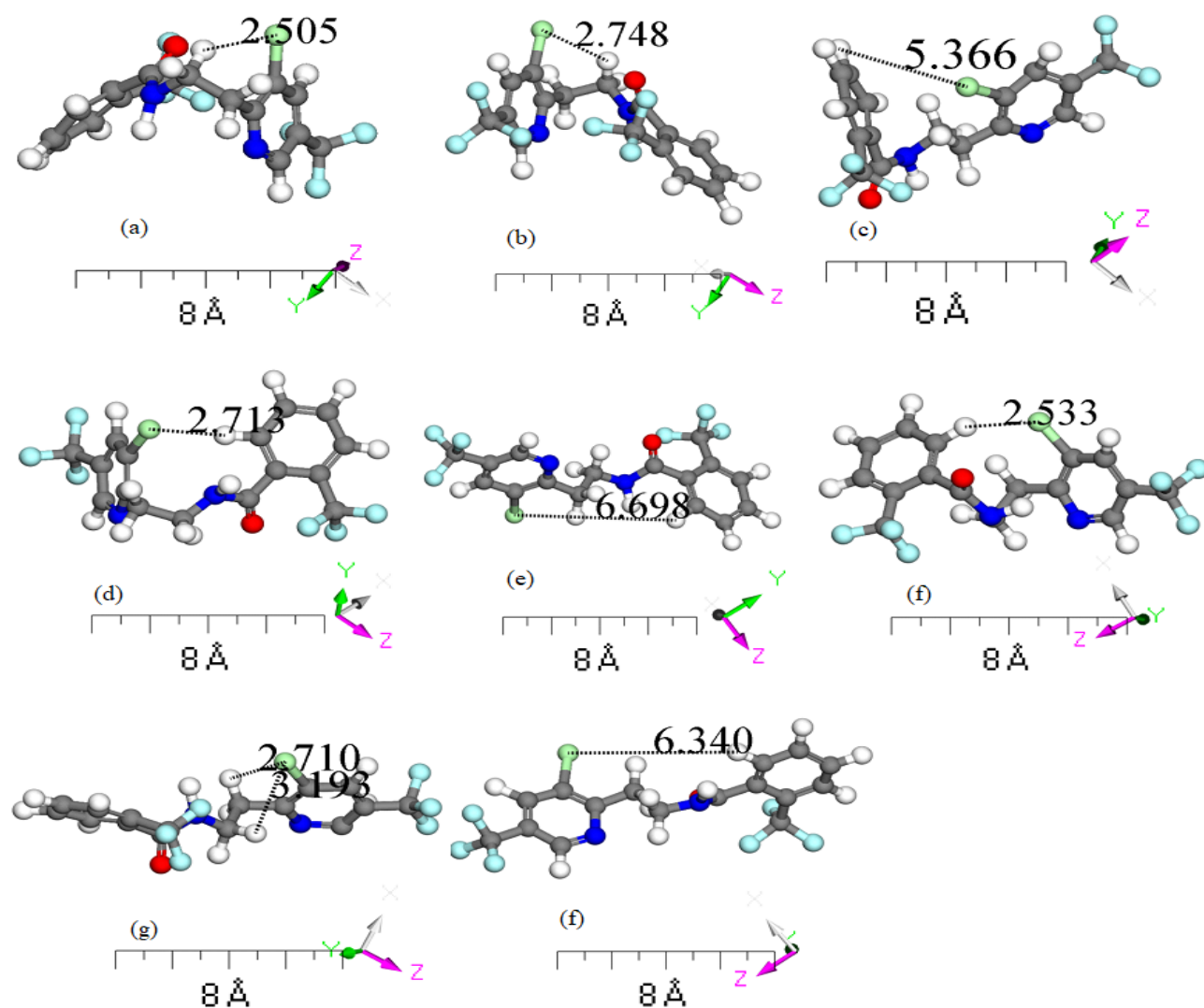


Fig. 4. Structural change of fluopyram in real water, result of AIMD simulation after 10 ns using DFT/GGA/PBE on the basis of DNP 4.4 level of theory. (No presented water molecular)

According to these results, we can infer that the TP V and TP VI were N-(2-[3-chloro-5-(trifluoromethyl)-2-ylidiny]ethyl)-2-trifluoromethyl-3-hydroxy) benzamide and N-(2-[3-chloro-5-(trifluoromethyl)-2-pyridinyl]ethyl)-2-trifluoromethyl-6-hydroxy) benzamide, respectively.

3.3. Ab initio molecular dynamics simulation

What is interesting about the data in this experiments is that the TP I was also identified one of the products in photocatalytic degradation of fluopyram. In our previous study, TP I was the main product of fluopyram photolysis and hydrolysis, and it was more stable to photolysis than fluopyram (Dong and Hu 2016). In present study, TP I was also identified in high field of 40% compared with fluopyram.

In general, therefore, it seems that the reaction of generating a cyclic organic compound (8 membered ring) at a room temperature does not occur easily. Moreover, as shown in Fig. 2, the bond length between Cl and noted H atom was 7.29 Å in the optimized structure of fluopyram. Therefore, these results need to be interpreted with caution.

So AIMD simulations were conducted to clarify this question. After 10 ps AIMD simulation, the structural change of fluopyram were shown in Fig. 4. As can be seen in Fig. 4, distance between Cl and noted H atom in (d), (f) were 2.713 and 2.533 Å, respectively. It was shown that the distance between Cl and noted H atom was significantly decreased to about 2.533-2.713 Å from initial distance of 7.373 Å. These distance was enough to formation the 8 membered cyclic compound (TP I) while away a HCl. According to these data, we are found that water molecular can be important role to structural change of fluopyram, therefore, it is possible to formation of the 8 membered cyclic organic compound under the room temperature while exist water.

3.4. Photocatalytic degradation path-way of fluopyram

The correlation between the irradiation time and the peak intensities recorded by the HPLC-MS/MS were shown in Fig. 5.

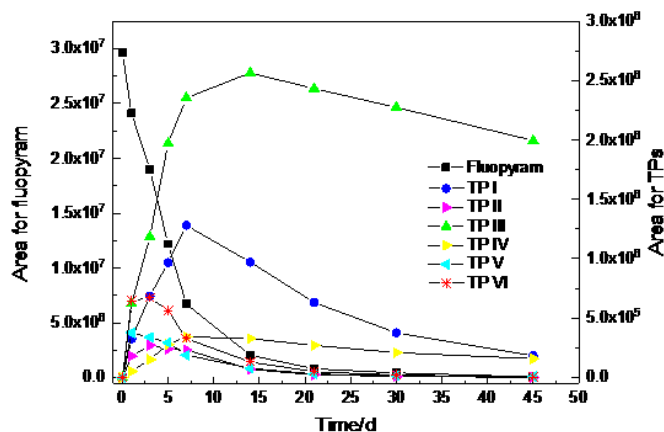


Fig. 5. Evolution profiles of fluopyram and its TPs

As shown in Fig. 5, TP III has maximum concentration at 14 d under the experiments condition. And TP I was found to be the secondary by product achieving its maximum concentration in 7 d, and then degraded slowly to achieve its trace level in 45 d. In our previous study, TP I was the main photoproduct of fluopyram photolysis and was more stable to photolysis than fluopyram (Dong and Hu 2016). The evolution profile indicated that the presence of TiO_2 not only accelerated degradation of fluopyram but also degradation of TP II, TP V and TP VI reached their maximum of concentration around 2-3 d and decreased progressively. Although TP IV was in trace level, its concentration was nearly invariable after 7 d, which indicated that it was more persistent than other TPs and fluopyram to the photocatalytic degradation.

On the basis of the above results and assumptions, a tentative pathway for the photocatalytic degradation of fluopyram was proposed in Fig. 6. The TPs formed in mainly three different pathways.

In the first case, pyridine-C1 bond was either the homolytic cleavage or heterolytic cleavage after photon-absorption. The homolytic cleavage of pyridine-C1 bond was strongly affected by stability of solvent. The more stable is the solvent, the higher the photo-dechlorination rate by homolytic pathway (Sevilla-Morán et al. 2014; Santos et al. 2016). TP I is at trace level (data not shown) in acetonitrile, an unstable solvent and hydrogen donor, after irradiating under UV-Vis, which indicate that pyridine-C1 bond was the homolytic cleavage and then intramolecular cy-

clization occurred during TP I formation. The formation of TP II was the nucleophilic substitution after heterolytic cleavage of the pyridine-Cl bond. The similar pathways have been reported in the study of triazine-based pesticides photolysis and polyhalogenated diphenyl ethers photodegradation (Canle et al. 2005; Santos et al. 2016).

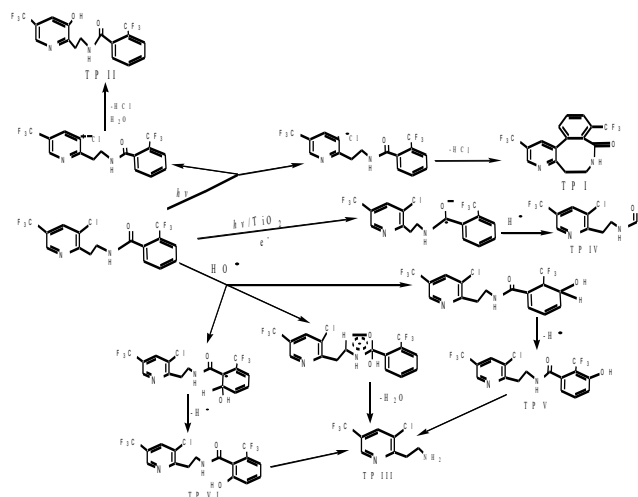


Fig. 6. Tentative pathways for photocatalytic degra

dation of fluopyram by TiO_2

In the second pathway, fluopyram may undergo the attack of the $-\text{OH}$ group in the benzene ring and loss of a proton, which results in the formation of TP V and TP VI. In the similar way, the OH group may also attack the carboxide of fluopyram, TP V and TP VI, which results in the formation of penta cyclic transient state. And then, the amido bond cleaves and TP III forms. Liang et al. (2010) have reported the formation of penta cyclic transient state in diphenamid degradation by photocatalysis with TiO_2/UVA . The evolution profiles of TPs also showed that TP V and TP VI possibly degrade to TP III (Fig. 6). In the last one, fluopyram could form the radical anion after obtaining one electron, which may undergo the loss of trifluorotoluene. Attack of a proton on the radical anion yields an identified intermediate TP IV.

Table 3 The toxicity prediction results of fluopyram and its products using ECOSAR

| Compounds | Acute toxicity (mg L^{-1}) | | | Chronic toxicity (mg L^{-1}) | | |
|-----------|---------------------------------------|-------------------------------------|----------------------------|---|--------------------------------------|----------------------------|
| | Fish (LC_{50}) | <i>Daphnia</i> (LC_{50}) | Algae (EC_{50}) | Fish (ChV_{50}) | <i>Daphnia</i> (ChV_{50}) | Algae (EC_{50}) |
| Fluopyram | 1.0 | 0.92 | 0.87 | 0.14 | 0.15 | 0.76 |
| TP I | 3.5 | 2.8 | 2.6 | 0.44 | 0.41 | 1.7 |
| TP II | 10 | 7.3 | 6.8 | 1.2 | 0.99 | 3.4 |
| TP III | 402 | 198 | 183 | 38 | 19 | 34 |
| TP IV | 617 | 295 | 273 | 57 | 28 | 48 |
| TP V | 2.9 | 2.4 | 2.2 | 0.36 | 0.36 | 1.5 |
| TP VI | 0.58 | 0.55 | 0.52 | 0.079 | 0.094 | 0.52 |

Table 4 The toxicity prediction results of fluopyram and its products using T.E.S.T.

| Compounds | Fish ^a | <i>Daphnia magna</i> ^b | Rats ^c | BCFs | DT | Mutagenicity |
|-----------|-------------------|-----------------------------------|-------------------|------|-----|--------------|
| Fluopyram | 0.29 | 0.14 | 1020 | 74 | Yes | No |
| TP I | 0.63 | 1.4 | 343 | 19 | Yes | No |
| TP II | 0.45 | 0.08 | 489 | 37 | Yes | No |
| TP III | 24 | 3.8 | 706 | 78 | Yes | No |
| TP IV | 9.15 | -- ^d | 1047 | 50 | Yes | No |
| TP V | 0.32 | 0.14 | 393 | 46 | Yes | No |
| TP VI | 0.32 | 0.25 | 486 | 50 | Yes | No |

^a 96 h- LC_{50} , mg L^{-1} ; ^b 48 h- LC_{50} , mg L^{-1} ; ^c Oral LD_{50} , mg kg^{-1} bw.

The toxicity prediction results for fluopyram and its TPs are presented in Table 3 and Table 4. As shown in Table 3, fluopyram and TP VI are highly toxic, TP I, TP II and TP V are moderately toxic, and TP III and TP IV are non-toxic for aquatic organism. As shown in Table 4, fluopyram and its TPs are toxic for aquatic organism.

Although the toxicity estimation values of oral rat LD₅₀ indicated a low toxicity for fluopyram and its TPs, all TPs were potentially more toxic than, or about as toxic as fluopyram. Moreover, the fungicide and its TPs were non-mutagenic while they showed the developmental toxicity and resistance to bioaccumulation. These data indicated that fluopyram and its TPs might cause damage to humans and wildlife. However, the oral rat LD₅₀ of fluopyram was >2000 mg kg⁻¹ (European Food Safety Authority 2011), which was much higher than the prediction value. In addition, fluopyram caused thyroid tumors and liver tumors (Rouquié et al. 2014; Tinwell et al. 2014). Therefore, *in vivo* and *in vitro* assays should be fulfilled in order to assess the toxicity of these compounds.

4. CONCLUSION

Six photolysis products of fluopyram in aqueous TiO₂ suspension including two products that was reported by previous our study were identified by HPLC-ESI-MS/MS and the quantum chemistry calculations. With the exception of TP I and TP II, the structures proposed for photolysis products have not been reported in previous studies. A degradation pathway was tentatively proposed based on the chemical structures and kinetics data. The toxicity predictions results showed that the TPs formed during photocatalytic degradation were potentially more toxic than fluopyram. Hence, a detailed and careful experimental ecotoxicological study of the TPs is needed to perform a suitable risk assessment.

ACKNOWLEDGMENTS:

This study was funded by the Fundamental Research Funds for the Central Universities (No.: FRF-TP-17-008A1) and Beijing Municipal Natural Science Foundation (No.: 8162029).

REFERENCES

- [1] Berberidou C, Kitsiou V, Karahanidou S et al (2015) Photocatalytic degradation of the herbicide clopyralid: kinetics, degradation pathways and ecotoxicity evaluation. *J Chem Technol Biot* 91(9): 2510-2518 [View Article](#)
- [2] Boxall A, Sinclair CJ, Kathrin F et al (2004) When synthetic chemicals degrade in the environment. *Environ Sci Technol* 38(19): 368A-375A [View Article](#)
- [3] Demircioğlu Z, Kaştaş ÇA, Büyükgüngör O (2015) Theoretical analysis (NBO, NPA, Mulliken Population Method) and molecular orbital studies (hardness, chemical potential, electrophilicity and Fukui function analysis) of (E)-2-((4-hydroxy-2-methyl- phenylimino)methyl)-3-methoxyphenol. *J Mol Struct* 1091:183-195 [View Article](#)
- [4] Dong BZ, Hu JY (2016) Photodegradation of the novel fungicide fluopyram in aqueous solution: Kinetics, transformation products and toxicity evolution. *Environ Sci Pollut R* 23(19): 19096-19106 PMID:27343079 [View Article](#) [PubMed/NCBI](#)
- [5] European Food Safety Authority (2011) Setting of new MRLs and import tolerances for fluopyram in various crops. *EFSA J* 9 (9): 2388 [View Article](#)
- [6] Frisch, M.J., Trucks, G.W., Schlegel, H.B., et al., Gaussian 09, Revision D.01, Gaussian, Inc, Wallingford, CT, 2013.
- [7] Govindarajan N., Tiwari A., Ensing B., Meijer E.J., Impact of ligand flexibility and solvent on the O-O bond formation step in a highly active Ru water oxidation catalyst, *Inorg. Chem.* (2018), PMID:29732882 [View Article](#) [PubMed/NCBI](#)
- [8] Govindarajan N., Sinha V., Bruin B. de, Meijer E.J., How solvent affects C-H activation and hydrogen production pathways in homogeneous Ru-catalysed methanol dehydrogenation reactions, *ACS Catal.* 8 (2018) 6908-6913. PMID:30101037 [View Article](#) [PubMed/NCBI](#)
- [9] Jung, H.W., Kang, J.H., Chun, H.J., Han, B.C., First principles computational study on hydrolysis of hazardous chemicals phosphorus trichloride and oxychloride (PCl₃ and POCl₃) catalyzed by molecular water clusters, *Journal of Hazardous Materials* 341 (2018) 457-463 PMID:28854386 [View Article](#) [PubMed/NCBI](#)
- [10] Koubský T, Fojtíková J, Kalvoda L (2017) Radical degradation stability of ether linkage in N,N,N',N'-tetraoctyldiglycolamide and related organic extractants: A density functional study. *Prog Nucl Energ* 94: 208-215 [View Article](#)

- [cle](#)
- [11] Liang HC, Li XZ, Yang YH et al (2010) Comparison of the degradations of diphenamid by homogeneous photolysis and heterogeneous photocatalysis in aqueous solution. *Chemosphere* 80(4): 366-374 PMID:20494398 [View Article](#) [PubMed/NCBI](#)
 - [12] Martínez Vidal JL, Plaza-Bolaños P, Romero-González R et al (2009) Determination of pesticide transformation products: A review of extraction and detection methods. *J Chromatogr A* 1216: 6767-6788 PMID:19720377 [View Article](#) [PubMed/NCBI](#)
 - [13] Monkhorst H.J., Pack J.D., Special points for Brillouin-zone integrations, *Phys. Rev. B: Condens. Matter Mater. Phys.* 13 (1976) 5188-5192. [View Article](#)
 - [14] Pavlova A., Meijer E.J., Understanding the role of water in aqueous rutheniumcatalyzed transfer hydrogenation of ketones, *ChemPhysChem* 13 (2012) 3492-3496. PMID:22927215 [View Article](#) [PubMed/NCBI](#)
 - [15] Perdew J.P., Burke K., Ernzerhof M., Generalized gradient approximation made simple, *Phys. Rev. Lett.* 77 (1996) 3865-3868. PMID:10062328 [View Article](#) [PubMed/NCBI](#)
 - [16] Peverati R, Truhlar DG (2012) M11-L: A local density functional that provides improved accuracy for electronic structure calculations in chemistry and physics. *J Phy Chem Lett* 3: 117-124 [View Article](#)
 - [17] Postigo C, Sirtori C, Oller I et al (2011a) Photolytic and photocatalytic transformation of methadone in aqueous solutions under solar irradiation: kinetics, characterization of major intermediate products and toxicity evaluation. *Water Res* 45: 4815-4826 PMID:21767861 [View Article](#) [PubMed/NCBI](#)
 - [18] Postigo C, Sirtori C, Oller I et al (2011b) Solar transformation and photocatalytic treatment of cocaine in water: kinetics, characterization of major intermediate products and toxicity evaluation. *Appl Catal B: Environ* 104: 37-48 [View Article](#)
 - [19] Rouquié D, Tinwell H, Blanck O et al (2014) Thyroid tumor formation in the male mouse induced by fluopyram is mediated by activation of hepatic CAR/PXR nuclear receptors. *Regul Toxicol Pharm* 70(3): 673-80 PMID:25455223 [View Article](#) [PubMed/NCBI](#)
 - [20] Santos MS, Alves A, Madeira LM (2016) Chemical and photochemical degradation of polybrominated diphenyl ethers in liquid systems - A review. *Water Res* 88: 39-59 PMID:26465809 [View Article](#) [PubMed/NCBI](#)
 - [21] Stamatis N, Antonopoulou M, Konstantinou I (2015) Photocatalytic degradation kinetics and mechanisms of fungicide tebuconazole in aqueous TiO₂ suspensions. *Catal Today* 252: 93-99 [View Article](#)
 - [22] Sevilla-Morán B, López-Goti C, Alonso-Prados JL et al (2014) Aqueous photodegradation of sethoxydim herbicide: Qtof elucidation of its by-products, mechanism and degradation pathway. *Sci Total Environ* 472: 842-850 PMID:24342090 [View Article](#) [PubMed/NCBI](#)
 - [23] Šojić DV, Anderluh VB, Orčić DZ et al (2009) Photodegradation of clopyralid in TiO₂ suspensions: identification of intermediates and reaction pathways. *J Hazard Mater* 168: 94-101 PMID:19264403 [View Article](#) [PubMed/NCBI](#)
 - [24] Šojić DV, Orčić DZ, Četojević-Simin DD et al (2014) Kinetics and the mechanism of the photocatalytic degradation of mesotrione in aqueous suspension and toxicity of its degradation mixtures. *J Mol Catal A-Chem* 392(10): 67-75 [View Article](#)
 - [25] Tinwell H, Rouquié D, Schorsch F et al (2014) Liver tumor formation in female rat induced by fluopyram is mediated by CAR/PXR nuclear receptor activation. *Regul Toxicol Pharm* 70 (3): 648-658 PMID:25305127 [View Article](#) [PubMed/NCBI](#)
 - [26] The Health Canada Pest Management Regulatory Agency (2014) Evaluation report- ERC 2014-02: fluopyram. 2-7
 - [27] Yang H, Li GY, An TC et al (2010) Photocatalytic degradation kinetics and mechanism of environmental pharmaceuticals in aqueous suspension of TiO₂: a case of sulfa drugs, *Catal Today* 53: 200-207 [View Article](#)
 - [28] Zhang Y, Xu J, Dong F et al (2014) Response of microbial community to a new fungicide fluopyram in the silty-loam agricultural soil. *Ecotox Environ Safe* 108C: 273-280 PMID:25105487 [View Article](#) [PubMed/NCBI](#)